

*Proceedings*  
*Advanced Materials for Construction of*  
*Bridges, Buildings, and Other Structures III*

---

Engineering Conferences International

Year 2003

---

Development of Space Truss Structure  
Using Glass Fiber Reinforced Plastics

Hiroya Hagio\*  
Koichiro Takahashi\*\*

Yoshikazu Utsumi†  
Go Itohiya††

Kohzo Kimura‡  
Hitoshi Tazawa‡‡

\*Obayashi Corporation, [hagio.hiroya@obayashi.co.jp](mailto:hagio.hiroya@obayashi.co.jp)

†Obayashi Corporation, [utsumi.yoshikazu@obayashi.co.jp](mailto:utsumi.yoshikazu@obayashi.co.jp)

‡Obayashi Corporation, [kimura.kohzo@obayashi.co.jp](mailto:kimura.kohzo@obayashi.co.jp)

\*\*Obayashi Corporation, [takahashi.koichiro@obayashi.co.jp](mailto:takahashi.koichiro@obayashi.co.jp)

††Asahi Glass Matex Co., Ltd., [itohiya@agm.co.jp](mailto:itohiya@agm.co.jp)

‡‡Asahi Glass Matex Co., Ltd., [tazawa@agm.co.jp](mailto:tazawa@agm.co.jp)

This paper is posted at ECI Digital Archives.

[http://dc.engconfintl.org/advanced\\_materials/11](http://dc.engconfintl.org/advanced_materials/11)

## Development of Space Truss Structure Using Glass Fiber Reinforced Plastics

Hiroya HAGIO<sup>1</sup>, Yoshikazu UTSUMI<sup>2</sup>, Kohzo KIMURA<sup>3</sup>, Koichiro TAKAHASHI<sup>4</sup>  
Go Itohiya<sup>5</sup>, Hitoshi TAZAWA<sup>6</sup>

**KEY WORDS:** Space Truss Structure, Buckling, Fire Protecting Performance, GFRP

### ABSTRACT

This paper describes the development of a space truss structure using Glass Fiber Reinforced Plastic (GFRP) pipe that decreases life cycle cost and enhances construction efficiency. Material tests, structural experiments and FEM analysis verify the practicality of this structural system.

### 1. INTRODUCTION

There has been increasing social demand to extend the life of buildings and to decrease their life cycle cost to reduce carbon monoxide emissions. Because of its durability, GFRP pipes are applied to space truss structures to reduce maintenance costs. Maintenance costs are expected to be reduced even in severe environments such as indoor pools, seashores and hot springs. Furthermore, GFRP's light weight is expected to result in shorter construction time. Fig.1 is a conceptual diagram of a space truss structure showing the name of each member.

---

<sup>1</sup> Deputy Chief Research Engineer, Project Promotion Department, Technical Research Institute, OBAYASHI Corporation, 4-640 shimokiyoto, Kiyose-shi, Tokyo 204-0011 Japan, T: 81-424-95-1019, hagio.hiroya@obayashi.co.jp

<sup>2</sup> Research Engineer, Construction System Engineering Department, Technical Research Institute, OBAYASHI Corporation, 4-640 shimokiyoto, Kiyose-shi, Tokyo 204-0011 Japan, T: 81-424-95-1135, utsumi.yoshikazu@obayashi.co.jp

<sup>3</sup> Dr.Eng., General Manager-In Charge, Project Promotion Department, Technical Research Institute, OBAYASHI Corporation, 4-640 shimokiyoto, Kiyose-shi, Tokyo 204-0011 Japan, T: 81-424-95-1120, kimura.kohzo@obayashi.co.jp

<sup>4</sup> Deputy Chief Research Engineer, Project Promotion Department, Technical Research Institute, OBAYASHI Corporation, 4-640 shimokiyoto, Kiyose-shi, Tokyo 204-0011 Japan, T: 81-424-95-1120, takahashi.koichiro@obayashi.co.jp

<sup>5</sup> Technical Group New Business Dept., ASAHI GLASS MATEX CO.,LTD. 1-2-27, Miyashimo, Sagamihara, Kanagawa 229-1112, Japan, T: 81-42-772-1174, itohiya@agm.co.jp

<sup>6</sup> General Manager C&A DEPARTMENT, ASAHI GLASS MATEX CO.,LTD. 1-2-27, Miyashimo, Sagamihara, Kanagawa 229-1112, Japan, T: 81-42-772-1174, tazawa@agm.co.jp

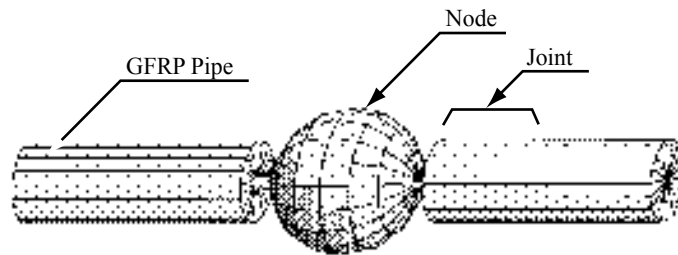


Fig.1 Conceptual Diagram of Space Truss Structure

## 2. MATERIAL PROPERTIES OF GFRP PIPES

GFRP pipe is made of E glass and modified acrylic resin (FR resin). The pipes are formed by the pultruded method. FR resin's characteristics include weather resistance, chemical resistance and incombustibility. The pipe used in these tests had an external diameter of 145mm and a wall thickness of 7.5mm. This cross section is determined by trial design. Sections 2.1 and 2.2 describe the material properties under room-temperature and high-temperature environments. Section 2.3 describes the material's fire protection performance.

### 2.1 Material Properties of GFRP at Room Temperature

Tensile and compressive tests were performed in accordance with JIS K 7054 shown in Fig.2 and JIS K 7056 shown in Fig.3. In addition, pipes 200mm long, as shown in Fig.4, were not cut in the longitudinal direction but the actual section was directly compressed. The results of tensile and compressive tests are shown in table 1. The compressive elastic modulus obtained by the JIS K 7054 tests is equivalent to that of direct compressive tests. However, the JIS K 7054 compressive strength is higher than that of compressive tests on the actual section. The compressive strength of the former is unreliable in comparison with the results of later-described buckling tests. It is likely that the supporting jig constrained the radial deformation. Accordingly, the compressive strength obtained from the direct compressive tests is adopted as the compressive strength in consideration of the dispersion.

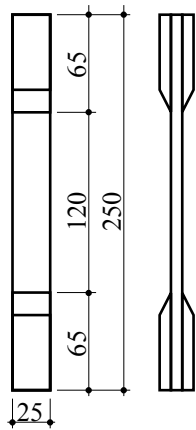


Fig.2 JIS K 7054

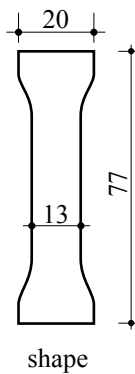


Fig.3 JIS K 7056

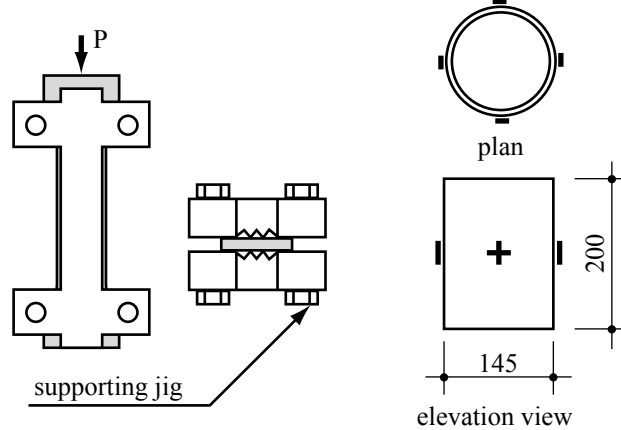


Fig.4 Method of suggesting

Table 1 Material Strength Test Results (\*: 200mm, \*\*: 290mm)

	JIS K 7054		JIS K 7056		with actual section*		with actual section**	
	$\sigma_t$ N/mm <sup>2</sup>	$E_t$ kN/mm <sup>2</sup>	$\sigma_c$ N/mm <sup>2</sup>	$E_c$ kN/mm <sup>2</sup>	$\sigma_c$ N/mm <sup>2</sup>	$E_c$ kN/mm <sup>2</sup>	$\sigma_c$ N/mm <sup>2</sup>	$E_c$ kN/mm <sup>2</sup>
1	294	19.9	212	24.4	195	25.6	190	25.7
2	388	22.7	230	25.7	211	25.9	210	25.4
3	301	17.6	217	29.2	173	25.9	172	25.4
4	286	21.1	217	25.3	-	-	190	26.2
5	337	20.2	233	22.5	-	-	179	26.2

## 2.2 Material Properties of GFRP at High Temperature

High-temperature strength tests were performed on GFRP at a preset temperature in a furnace. The results of high-temperature strength tests are shown in Fig. 5. The tensile strength at 250 degrees was approximately 80% of that at room temperature. The compressive strength at 175 degrees was about 70% of that at room temperature. It therefore appears that the inflection point, where the strength drops rapidly, is beyond the scope of these tests.

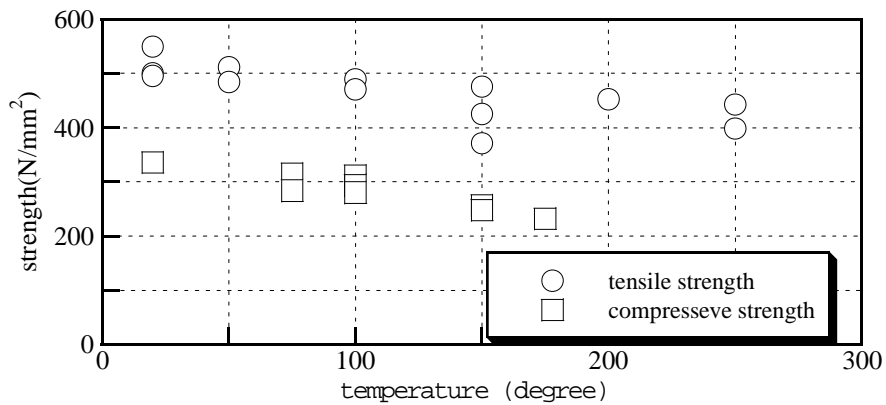


Fig.5 Strength of GFRP at High Temperatures

### 2.3 Fire Protection Performance of GFRP

The fireproof performance of FR resin is compared with that of phenol resin (PR resin). The test samples were 100mm square and 12.5mm thick. The tests were performed in accordance with ISO 5660. Table 2 shows the results, and Fig.6 and 7 illustrate the relationships between the heat release rate and time and the relationships between the smoke extinction coefficient and time. According to Fig.6, PR resin corresponded to a flame retardant material. However, the ignition time and the quench time of the FR resin were equal to those of the PR resin. But the maximum heat release rate of the FR resin was one fifth that of the PR resin. Furthermore, the gross calorific value of the FR resin was much smaller than that of the PR resin. Thus, the FR resin is suitable as a quasi-noncombustible material. Furthermore, we see from Table 2 that the amount of smoke for the FR resin was less than that of the PR resin. Consequently, it is clear that the FR resin is superior to the PR resin in respect of fireproof performance.

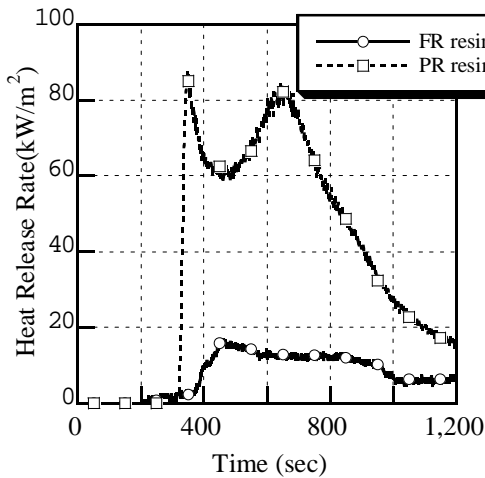


Fig.6 Relationships between Heat Release Rate and Time

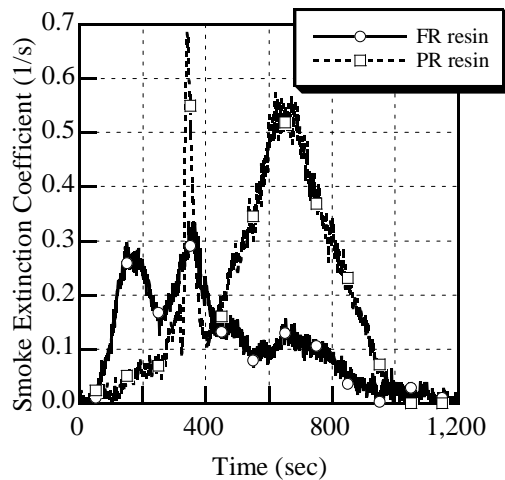


Fig.7 Relationships between Smoke Extinction Coefficient and Time

Table 2 Results of Cone-Calorimeter

name	ignition time	maximum heat release rate	time at extinction of flame	gross calorific value MJ/m <sup>2</sup>			judgement
				5min	10min	20min	
	sec	kW/m <sup>2</sup>	sec				
FR resin	389	16.7	1000	0.1	3.2	9.0	quasi-noncombustible
PR resin	323	87.3	1120	0.0	18.3	44.9	flame retardant

### 3. STRUCTURAL PERFORMANCE OF EACH MEMBER

In order to clarify the structural performance of a truss member, a joint member and a node member, experiments were performed on each.

### 3.1 Structural Performance of Truss Member

Compressive tests were carried out on GFRP pipes to determine crushing failure for a small slenderness ratio and buckling failure for a large slenderness ratio. The parameter was length. Test pieces were 1000mm to 3000mm long in 500mm steps. Three pieces of each length were tested. Both ends were pin supported. Four strain gauges were joined with an adhesive at the central part as shown in Fig.3. The relationships between axial stress and axial strains for the pipe length 2500mm are shown in Fig.8. This graph shows that the specimen crushes after elastic buckling. The results of compression test on the pipes are plotted up to failure in Fig.9. The slenderness ratio is calculated as the distance from pin support to the other support. Fig.9 shows Euler's equation calculated from material tests and the results of the compressive tests with the actual section. The experimental values are similar to those given by Euler's equation. Furthermore, the fluctuation of the tests is small. Thus, the buckling stress is demonstrated by Euler's equation calculated from material tests. The compressive stress was evaluated not by JIS K 7056 compression test results, but rather by compressive tests on the actual section to take dispersion into account.

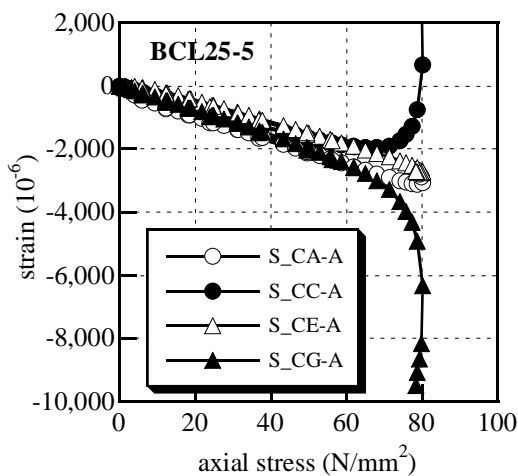


Fig.8 Relationships between Axial Stress and Axial Strains of Pipe length 2500mm

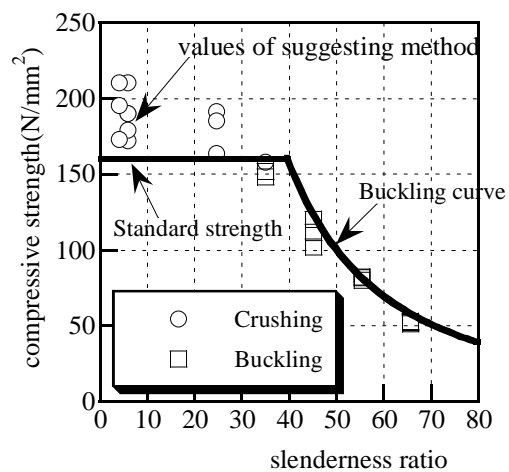


Fig.9 Results of Compression Tests on Pipes

### 3.2 Structural Performance of Joint Member

Compressive and tensile tests were performed to clarify the structural performance of a joint. Fig.10 illustrates its suggested structure. The inner pipe and the GFRP pipe are connected with rivets as well as adhesive. The load/displacement relationships are shown in Fig.11.

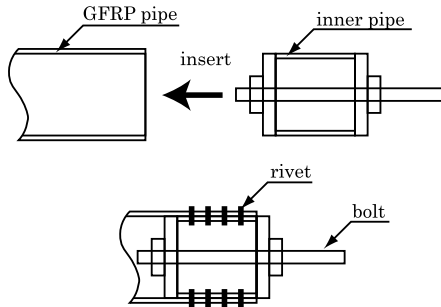


Fig.10 Joint Structure

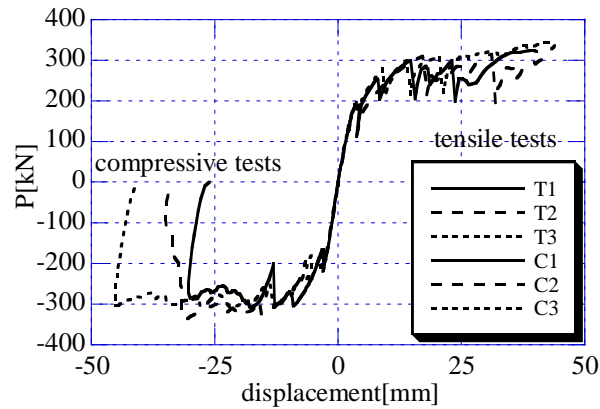


Fig.11 Load/Displacement Relationships

### 3.3 Structural Performance of Node Member

Compressive and tensile tests were carried out to clarify the structural performance of the stainless steel node. Due to space limitations, discussion on the results of the tensile tests is limited here. The load/displacement relationships are shown in Fig.12. The heavy line in Fig.12 is the calculated value assuming symmetry. It is discovered that the rigidity obtained from the test is close to calculated one.

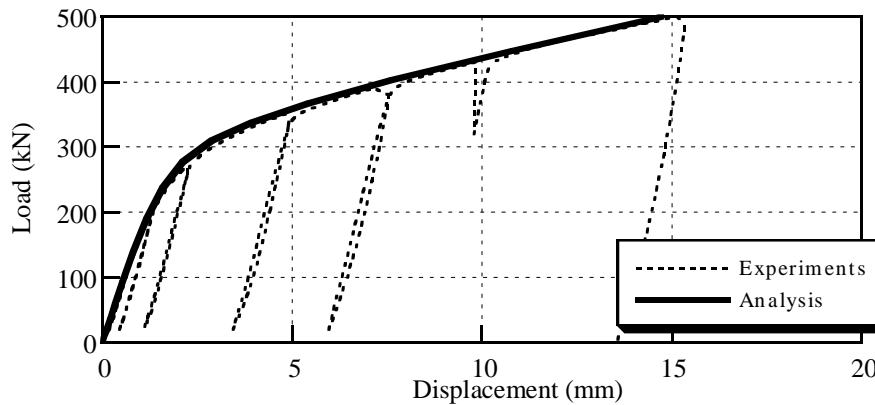


Fig.12 Load/Displacement Relationships

## 4. EXPERIMENT ON SPACE TRUSS STRUCTURAL FRAME

This chapter describes the structural performance of a space truss structural frame combining each member.

### 4.1 Specimen

The size of the specimen was based on the trial design of the 10m×20m span. The specimen comprises three quadrilaterals connected at two upper chords. From the design axial force of the truss member of 150kN, the GFRP pipe has an external

diameter of 145mm and a wall thickness of 7.5mm. The bolts are made of SUS630. The nodes are made of SUS304A.

#### 4.2 Experimental Method

Photo.1 shows a view of the test. The test load was applied at the center of the four pin supports. The load, displacements and strains of the pipes were measured.

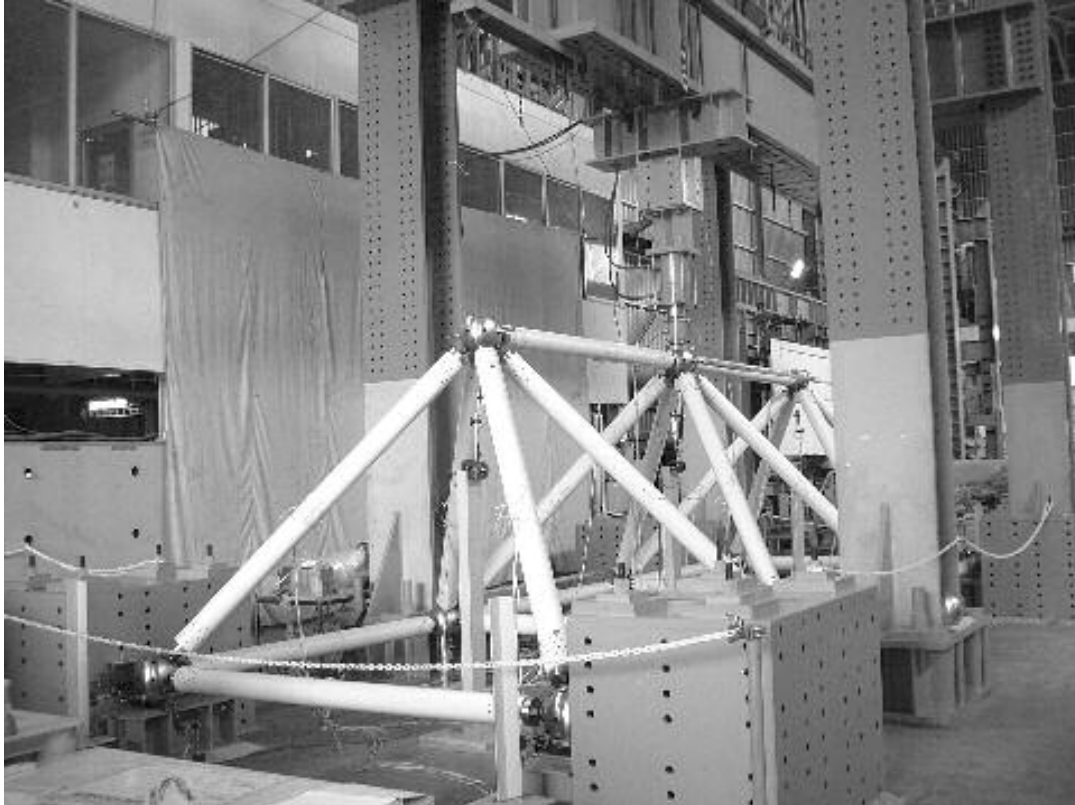


Photo.1 View of Test

#### 4.3 Results of the Experiment

Fig.13 shows the load/displacement relationships of points V10 and V11. The displacements are commensurate with the load. The maximum strength is determined by the buckling of the upper chord. Fig.14 show the upper chord load/strain relationships. Buckling is observed at 315kN. The maximum strength is 350kN. After that, the load drastically decreased. The buckling mode is antisymmetric, protruding from the vertical plane.



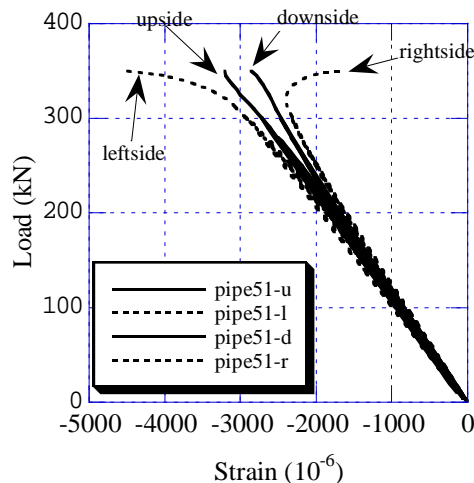
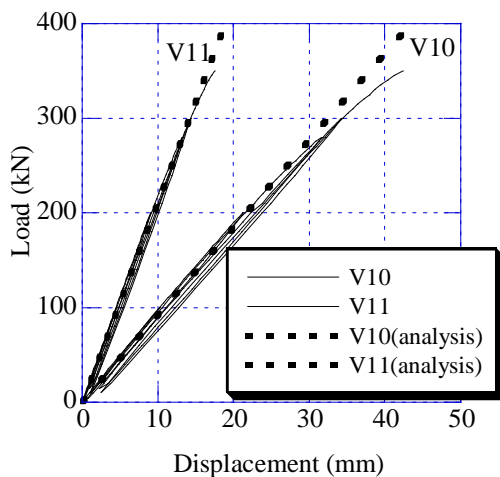


Fig.13 Load/Displacement Relationship      Fig.14 Upper Chord Load/Strain Relationship

#### 4.4 FEM analysis

Fig.15 shows the nodal numbers and the element numbers used for the FEM analysis. In Fig.15 the parentheses indicate the nodal point number. The equivalent rigidity of the component was calculated by linking the node, the bolt, the disk and the pipe as the serial spring. As a result, the compressive rigidity of the component is 31.2kN/mm<sup>2</sup>. The tensile rigidity is 29.4kN/mm<sup>2</sup>. The difference is due to the difference of the stress transmission path. Although the tensile elastic modulus is a little different from the compressive elastic modulus, the tensile elastic modulus is adopted for the FEM analysis on the ground so that the displacement calculated from the tensile elastic modulus is on the safe side. The deformation and the axial force when the load is 200kN in the analysis are shown in Fig.16. Then the vertical displacement at the center of the upper chord is 22mm. A glance at Fig.13 will reveal that the load/displacement relationship is equivalent to the experimental value of until the load reaches 280kN. Table 3 compares the axial force at a load of 200kN. Except where the axial force is small, the analytical values are similar to the experimental ones.

Table 3 Comparison of the Axial Force at Load 200kN

Number	Analysis	Experiment		ratio	Number	Analysis	Experiment		ratio
	Axial force	Strain	Axial force			Axial force	Strain	Axial force	
1	35.6	441	35.3	1.01	23	-70.3	-892	-72.8	0.97
2	105.7	1,443	115.5	0.92	24	69.7	922	73.8	0.94
3	35.6	448	35.9	0.99	31	-70.8	-903	-73.7	0.96
4	35.6	432	34.6	1.03	32	-70.8	-863	-70.5	1.00
5	105.7	1,399	112.0	0.94	33	-70.8	-906	-74.0	0.96
6	35.6	440	35.2	1.01	34	-70.8	-872	-71.2	0.99
7	0.0	62	5.0	0.00	41	-70.3	-847	-69.2	1.02
8	0.5	4	0.3	1.67	42	69.7	907	72.6	0.96
9	0.5	5	0.4	1.25	43	69.7	923	73.9	0.94
10	0.0	170	13.6	0.00	44	-70.3	-894	-73.0	0.96
21	69.7	893	71.5	0.97	51	-140.5	-1,797	146.7	-0.96
22	-70.3	-866	-70.7	0.99	52	-140.5	-1,767	-144.3	0.97

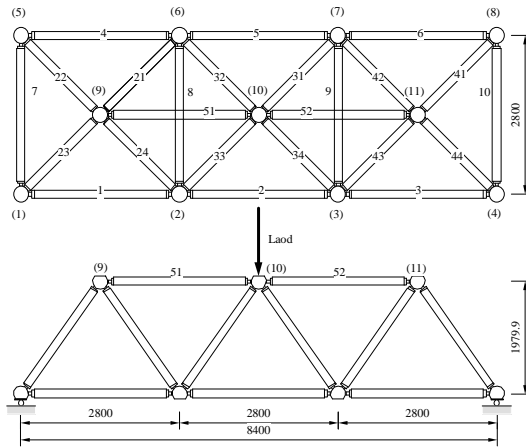


Fig.15 Nodal Numbers and Element Numbers

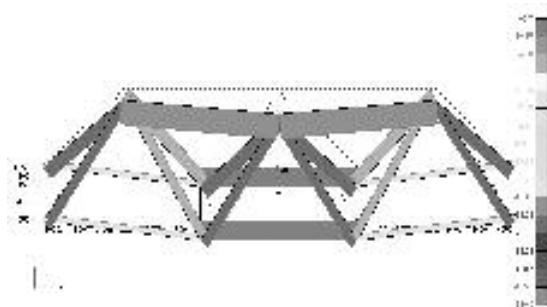


Fig.16 Displacement and Axial Force at Load 200kN

## 5.CONCLUSIONS

The conclusions of this paper are as follows:

1. The tensile strength and elastic modulus of the GFRP pipe are demonstrated by the method with JIS K 7054. The compressive strength and elastic modulus of the GFRP pipe are evaluated not by JIS K 7056 but rather by compressive tests with an actual section in consideration into the dispersion.
2. The modified acrylic resin is superior to the phenol resin in respect of fireproof performance.
3. An experiment was carried out on a space truss structural frame combining each member. As a result, the load/displacement relationship is linear until buckling occurs. Furthermore, the analytical values are similar to the experimental ones.

## REFERENCES

Yoshikazu Utsumi, Hiroya Hagio, Kohzo Kimura, Koichiro Takahashi, "Development of Space Truss Structure using Glass Fiber Reinforced Plastics (Part 1) -Studies on Structural Properties-", Report of Obayashi Corporation Technical Institute, No.65, 2002, pp11-16 (in Japanese)

Hiroya Hagio, Yoshikazu Utsumi, et al, "Development of Long Span Structure using Glass Fiber Reinforced Plastics (Part 1 and Part 2)", Summaries of Technical papers of Annual Meeting Architectural Institute of Japan, pp.963-966, 2000.9 (in Japanese)

Yoshikazu Utsumi, Hiroya Hagio, et al, "Development of Long Span Structure using Glass Fiber Reinforced Plastics (Part 3 and Part 4)", Summaries of Technical papers of Annual Meeting Architectural Institute of Japan, pp.871-874, 2001.9 (in Japanese)